Slits Affect the Timely Migration of Neural Crest Cells via Robo Receptor

Dion Giovannone, **Michelle Reyes**, **Rachel Reyes**, **Lisa Correa**, **Darwin Martinez**, **Hannah Ra**, **Gustavo Gomez**[$], **Josh Kaiser**, **Le Ma**[#], **Mary-Pat Stein**, and **Maria Elena de Bellard**[*]
California State University Northridge, Biology Dept., MC 8303. 18111 Nordhoff Street. Northridge, CA 91330

[#]Zilkha Neurogenetic Institute. KSOM of USC. 1501 San Pablo St. Los Angeles, CA 90033

[$]Division of Biology, 139-74. California Institute of Technology, Pasadena, CA 91125

SUMMARY

Background—Neural crest cells emerge by delamination from the dorsal neural tube and give rise to various components of the peripheral nervous system in vertebrate embryos. These cells change from non-motile into highly motile cells migrating to distant areas before further differentiation. Mechanisms controlling delamination and subsequent migration of neural crest cells are not fully understood. Slit2, a chemorepellant for axonal guidance that repels and stimulates motility of trunk neural crest cells away from the gut has recently been suggested to be a tumor suppressor molecule. The goal of this study was to further investigate the role of Slit2 in trunk neural crest cell migration by constitutive expression in neural crest cells.

Results—We found that Slit gain-of-function significantly impaired neural crest cell migration while Slit loss-of-function favored migration. In addition, we observed that the distribution of key cytoskeletal markers was disrupted in both gain and loss of function instances.

Conclusions—These findings suggest that Slit molecules might be involved in the processes that allow neural crest cells to begin migration and transitioning to a mesenchymal type.

Keywords

neural crest; cell migration; cell motility; Slit2; cytoskeleton

INTRODUCTION

The neural crest is a population of migrating cells that originate from the dorsal neural tube during vertebrate development that differentiate into many cell types. In order to migrate, neural crest cells need to change from an epithelial, non-motile cell type to a mesenchymal, highly motile cell type as they delaminate from the neural tube. This transformation is known as EMT for epithelial to mesenchymal transition, and is accompanied by changes in transcription factors, cell adhesion molecules and the cytoskeleton (Vernon and LaBonne, 2004; Taneyhill et al., 2007; Salvador et al., 2009; Thiery et al., 2009).

Although we know some of the key players in neural crest EMT transition, i.e. Slug, Sox9, Wnt, etc. there are still some fundamental aspects that still remain unanswered. Which key molecules do these transcription factors regulate? Which ones are key in starting or preventing neural crest delamination? How do these molecules regulate the precise timing of

[*]Corresponding author: Telephone: 818-677-6470, FAX: 818-677-2034, maria.debellard@csun.edu.

neural crest EMT transition? One family of molecules stands out among a list of candidates for their ubiquity in expression throughout neural crest development: Slits. These receptors and their ligands are present at the beginning of neural crest delamination, during and at the end of migration (De Bellard et al., 2003; Jia et al., 2005; Shiau et al., 2008; Shiau and Bronner-Fraser, 2009).

The Slit proteins (1, 2 and 3), have been known as key players in axonal guidance in both vertebrates and invertebrates (Brose et al., 1999; Kidd et al., 1999; Li et al., 1999), as well as guiding neural crest cells during migration (De Bellard et al., 2003; Jia et al., 2005). Slit glycoproteins function as repulsive factors during migration of neurons and glia (Hu, 1999; Wu et al., 1999; Kinrade et al., 2001) and can also regulate axon elongation/branching in mammals (Wang et al., 1999). But what is more interesting is that Slits and their Robo receptors have been found to play a role in cancer metastasis (Schmid et al., 2007; Sharma et al., 2007; Singh et al., 2007; Prasad et al., 2008; Tseng et al., 2010). More specifically, Slit molecules have recently been defined as true tumor suppressor molecules (Dallol et al., 2002; Dallol et al., 2003a; Dickinson et al., 2004; Yu et al., 2010). Slit expression correlated with reduced cell motility in cancer cells while reduced Slit expression is associated with more aggressive cancer types. Furthermore, Slit2 was found to regulate beta-catenin expression, critical during cell migration transitions (Kim et al., 2008; Prasad et al., 2008; Tseng et al., 2010). Altogether these data suggested that Slit-Robo interactions, present throughout crest development may not only play a role in their guidance, but may also affect their migratory transitions (Prasad et al., 2008; Tseng et al., 2010).

In this study, we examined the potential role of Slit in the process of neural crest cell migration. Slits are expressed in the dorsal neural tube by pre-migratory neural crest cells; however, expression decreases after emigration while Robo receptor expression increases. We tested the possible functional role of Slit on neural crest cell migration in vivo and in vitro using Slit gain of function and loss of function experiments. The results reveal for the first time a new role for Slit2 in neural crest cell migration and provide evidence for the ability of Slits to affect the timely migration of neural crest cells in a Robo-dependent manner.

RESULTS

Distribution of Slit expression during trunk neural crest migration

Slit molecules are known chemorepellants typically expressed along the pathways of growing axons (Kidd et al., 1999). In addition to axonal pathfinding, Slit molecules also guide migrating neural crest cells (De Bellard et al., 2003; Jia et al., 2005; Shiau et al., 2008). However, Slit molecules are not only expressed along the pathways that neural crest cells avoid but also are expressed by neural crest cells prior to migration away from the neural tube (Holmes and Niswander, 2001; De Bellard et al., 2003; Jia et al., 2005).

Neural crest cell induction occurs much earlier in chicken embryos than developmental stage HH17 when the peak of trunk crest migration takes place. However, it was not clear if Slits are expressed during earlier stages, before trunk neural crest initiates delamination (before HH13). We observed that in HH12-13, (Fig. 1A-C, H-K) as for HH17 (Supplementary Fig. 1A–H), Slit1, Slit2 and Slit3 are expressed in the trunk dorsal neural tube but are absent in the first wave of migrating trunk crest cells. By comparison, Slit receptor Robo1 is expressed in the closing neural tube and proximal somites, while Robo2 is expressed in an almost non-overlapping pattern to Robo1 in the caudal hindbrain and less prominently in the dorsal neural tube (Fig. 1D–E, L and Supplementary Fig. 1I–N). This stage comprises the peak of cranial neural crest migration as shown by Sox10 in situ (Fig. 1F–G, N–O) and trunk neural crest migration will not start until HH14 (Thiery et al., 1982;

Serbedzija et al., 1989). Therefore, pre-migratory trunk neural crest cells express both ligands and receptors before they begin to migrate. Later, during the peak of trunk neural crest cell migration (HH16-17), pre-migratory neural crest cells express Slits while the migrating neural crest expresses Robo (Supplementary Fig. 1) (De Bellard et al., 2003; Jia et al., 2005).

Slit expression was never observed in migrating trunk neural crest cells, only in the dorsal neural tube where pre-migratory trunk neural crest cells reside before the initiation of delaminating and subsequent migration. Towards the end of trunk neural crest cell migration (HH21), Slit1 and 2 continued to be expressed in the dorsal and ventral neural tube (Supplementary Fig. 1B, D, F, H). On the other hand, Robo1 and Robo2 have overlapping pattern of expression at these stages: both are expressed by the migrating trunk crest at HH17 (Supplementary Fig. 1I, K, M, O) and later on expressed in the dorsal root ganglion (Supplementary Fig. 1J, L, N).

Ectopic expression of Slits in trunk neural tube impairs neural crest cell migration

This fine tuning of Slit and Robo expression suggested that Slit molecules may have another role during neural crest cell development besides being a repellant for ventrally migrating trunk neural crest cells (De Bellard et al., 2003). Since Slit1 and/or Slit2 can impair metastatic cell migration (Tseng et al., 2010; Yu et al., 2010), we explored the possibility that Slits could also affect neural crest cell migration. We first approached this question by constitutively expressing Slit2 in gain-of-function (GOF) experiments. We hypothesized that Slit molecules have an analogous role in neural crest cells as in metastatic cells, preventing movement and affecting migratory capabilities.

We investigated this correlation by electroporating chicken embryo neural tubes at HH14-16, before the peak of trunk neural crest cell migration (HH16-17) with Slit either myc-tagged Slit or in a bi-cistronic plasmid. We observed that embryos electroporated with a control GFP-expressing plasmid displayed many GFP-positive cells that had migrated out of the neural tube along the ventromedial pathway (Fig. 2A and C) and that had already begun entering the hindlimb at 48 hours post electroporation (hpe). Comparatively, when mSlit1 or hSlit2 proteins were ectopically expressed in the neural tube, the regular pattern of neural crest cell migration along the ventromedial pathway was impaired (Fig. 2B and D for hSlit2 and data not shown for mSlit1) as well as the dorsomedial (arrowheads in Fig. 2D). This altered migration was observed at both 24 and 48 hpe and in 45/51 and 12/15 total embryos respectively, indicating that the migratory properties of the neural crest cells were not just impaired during their initial migration phase but remained impaired for the duration of hSlit2 expression. Cross sections of these embryos showed that while control neural crest cells expressing control GFP followed their normal ventro-medial pathway into dorsal aorta region, there were far fewer Slit-expressing cells that reached the dorsal aorta region in the Slit GOF electroporated embryos (Fig. 2E–F). This impaired migration was observed using either a myc-tagged Slit2 or using a bi-cistronic GFP plasmid for Slit2 expression.

The first wave of migrating neural crest cells in the trunk encompasses the cells that will eventually form the sympathetic ganglia by the dorsal aorta (Serbedzija et al., 1989). Thus, any sympathetic ganglia size reduction is an indication that either neural crest cells did not migrate properly or that the neural crest cells died en route to their destination. When we quantified the total number of electroporated cells in condensing dorsal root ganglion (DRG) and sympathetic ganglia (Table I), we found a significant reduction in the number of mSlit1 or hSlit2 expressing cells compared to controls. This deficit was especially marked for the sympathetic ganglia after mSlit1 GOF: 50%, $p<0.0005$ for DRG and 64%, $p<0.005$ for sympathetic ganglia. To determine whether or not cell death was responsible for the reduced number of Slit1-expressing cells in the ganglia, we scored the number of DAPI-stained

condensing or fragmented nuclei in the mSlit1 GOF compared with control GFP and did not find any significant difference (data not shown). TUNEL assays were also performed on these embryos and no increase in the amount of cell death was observed in Slit GOF compared to control or non-electroporated sides (data not shown). These results suggested that the reduction of Slit-expressing neural crest cells in DRG and sympathetic ganglia was not due to cell death but instead to impaired migration upon constitutive expression of Slit.

The size of neural crest cell derived structures depends on the cell cycle of migrating neural crest cells as well as the ongoing generation of neural crest cells from the dorsal neural tube, the latter of which is dependent on the timely and proper expression of pre-migratory neural crest cell transcription factors (Gammill and Bronner-Fraser, 2003). When we examined the expression of Pax7, Msx, Sox10 or Cad6b after ectopic expression of hSlit2 and mSlit1 in the neural tube, we did not observe any changes in the boundary or levels of expression of these molecules (data not shown). These results further suggested that the change in cell numbers we observed in Slit-expressing neural crest cells could be due to delay in delamination of neural crest cells still expressing high levels of Slits.

Slit Over-expression Impairs Cell Migration in vitro

The absence of Slit expression has been related to metastasis and notably the ectopic expression of Slit can impair tumor formation (Dallol et al., 2002; Dallol et al., 2003a; Dickinson et al., 2004). To further confirm that Slit GOF similarly affects neural crest cell migration, we performed in vitro experiments to reduce the influence of other guidance molecules during migration. Neural crest cell migration begins 2–3hrs after the neural tubes are introduced into in vitro culture. To eliminate neural crest cells that had undergone delamination immediately prior to the time of electroporation, electroporated neural tubes were explanted 5 hours post electroporation (hpe) into in vitro culture. In doing so, any GFP or myc-positive cells observed in the halo of neural crest cells correspond to cells that had continuous expression of Slit throughout the delamination process.

Observation of neural crest halos suggested that control GFP transfected cells migrated in larger numbers and longer distances from the neural tube explants than those from mSlit1 electroporated neural tubes (see control neural crest halo in Fig. 2G). Comparatively, we observed that mSlit1 electroporated neural crest cells had significantly smaller halos (observed in 80% of neural tubes, N= 45); had more rounded cells; and, had fewer plasmid expressing cells around the edge of the halo (Fig. 2H) compared with control GFP-expressing cells (Fig. 2G, N=96). We repeated this experiment with hSlit2-GFP and observed the same results: neural crest cells did not migrate as far away from the neural tube as control cells expressing GFP (N= 50, and data not shown). Once again, these findings with both Slit1 and Slit2 suggested that Slit over-expressing cells were either dying, changing their shape, or not emigrating from the neural tube. The possibility of cell death in Slit-positive cells was considered unlikely as we repeated these experiments in vitro and did not observe any difference in cell death between control and mSlit1 or hSlit2-expressing cells using the TUNEL assay (data not shown). In addition embryo sections co-stained with DAPI were analyzed for the presence of nuclear fragmentation or condensation, a sign of cell death. No significant differences between Slit-positive cells and non-electroporated neural crest cells were observed (data not shown). Taken altogether the in vivo and in vitro findings we can discard cell death as an effect of Slit GOF.

Neural crest cells derived from Slit electroporated neural tube and then cultured exhibited changes in cell morphology in both whole embryos and in cultures. Specifically, Slit-expressing cells were smaller in size and more rounded than non-Slit-expressing cells. We examined this more thoroughly by scoring for the number of cells in these cultures displaying a classic migratory shape versus a non-migratory rounded shape (Strachan and

Condic, 2003) and found that Slit1- or Slit2-expressing cells were more likely to be rounded (~70%). Furthermore, Slit-expressing cells rarely showed the classic stretched shape of migrating neural crest cells (Fig. 3A, N=500).

To ensure that electroporation and cytotoxicity due to high plasmid loads did not cause the rounded phenotypes we observed, experiments using chemical transfections of dissected neural tubes with the same plasmids were performed. Cell morphology was assessed by analyzing the total area covered by GFP- or Slit-GFP-expressing cells after 24hrs of culture. We observed that neural crest cells expressing Slit2 were smaller and rounder than control GFP-expressing cells (Fig. 3A, B). Figure 3B and C shows that Slit2-expressing cells were 73% the size of control cells (a ~25% size reduction, p<0.005, N>600 cells per treatment), indicating that Slit2 expression affected cell size. To discount any transfection artifact, we repeated these experiments using Macrophage inhibitory factor (GFP-MIF) as a positive control because it is known to enhance directional cell migration of leukocytes and we have found that is a neural crest cell chemoattractant (data not shown and personal communication) (Gregory et al., 2006). Cells expressing MIF were bigger and the percentage of cells with the migratory shape was increased compared to control cells, (Fig. 3C). In contrast, Slit molecules had the opposite effect, causing rounding of neural crest cells and reducing their ability for migration. Further confirmation of these morphological differences was obtained by measuring the long and short axis of neural crest cells. We found that Slit-expressing neural crest cells have a 2.24 ratio of long versus short axis compared with a 3.12 for control GFP (p<0.0004 T-test, N=60 cells per each treatment). Taken together, these results strongly suggest that Slit expression causes cell rounding and morphological alterations consistent with a non-migratory phenotype.

In order to observe the behavior of live cells following Slit electroporation, neural crest cells were imaged using confocal microscopy over a 2–3 hrs time course. We found that hSlit2-GFP cells rounded and stretched intermittently as well as exhibiting more membrane blebbing than controls (Fig. 4 and Supplementary Movie 1, 2). This behavior was observed at a 3:1 ratio in Slit2-expressing cells compared with control GFP-expressing cells in more than 10 movies per each treatment (Supplementary Movie 2 and data not shown). Tracing the paths of these GFP-expressing cells demonstrated that neural crest cells expressing Slit2-GFP had more stalls and short side turns along their paths compared with control GFP-expressing cells (Fig. 4E, arrows in J). The dynamic nature of these changes as observed in live cell imaging explains our observation of rounded, non-migratory and migratory phenotypes in cell culture.

Ectopic expression of Robo in trunk neural tube impairs neural crest cell migration

Neural crest cells express reduced amounts of Robo receptors prior to EMT transition. Once migration commences, Robo1 expression is dramatically up-regulated and Slit expression is down-regulated (De Bellard et al., 2003). Here, we assessed if the aberrant neural crest cell migration associated with Slit GOF was linked to the concomitant expression of Robo receptor by neural crest cells. Using electroporated Robo plasmids in HH15-16 neural tubes we examined the effect of Robo GOF after 24 and 48 hpe in neural crest cells. Robo1 GOF prevented neural crest migration more dramatically than Slit-expression GOF (observed in 90% of embryos, N=45) (Fig. 5B). In some embryos, no cell migration was observed (Fig. 5D). This result was confirmed by examination of embryo cross-sections following the electroporation of Robo plasmid confirming that very few neural crest cells migrated from the neural tube after Robo GOF compared with control GFP (Fig. 5E-F, N=12). We observed normal spinal nerves in these sections, implying that ventral motor axon elongation was not affected while neural crest cell migration was significantly impaired. A similar effect was observed when culturing electroporated neural tubes: fewer neural crest cells expressing Robo1 migrated all the way to the edge of the neural crest cell halo (Fig. 5H)

compared with control GFP-expressing neural tubes (Fig. 5G). This suggests that impaired migration was directly related to the expression of Robo1.

When we measured the difference in total area covered by neural crest cells positive for Slit or Robo compared to control electroporated cells we found that the total area covered by cells expressing Robo1 (56%), mSlit (65%) or hSlit2 (61%) was reduced compared with control GFP-expressing neural tubes (88%, p<0.005, >N=25 neural tubes per treatment) (Fig. 6A, B). Therefore, GOF expression of either Slit or Robo impaired neural crest cell migration.

Slit silencing enhanced neural crest cell migration in trunk neural tube

To further address the role of Slit molecules in neural crest cell migration, we performed loss-of-function (LOF) experiments using chicken Slit2 FITC-labeled morpholinos in HH13-14 chicken embryo neural tubes. We examined neural crest cell migration patterns following morpholino knock-down of Slit2 18 hpe. Slit2 LOF enhanced neural crest cell migration. Neural tubes expressing chicken Slit2 spliced blocking morpholinos (SpSlit2-MO) or Slit2 translational blocking morpholinos (TrnSlit2-MO) at the level of the last somites compared to cells expressing Slit2 spliced scrambled (SpCont-MO) or standard control morpholinos consistently demonstrated enhanced migration (Fig. 7A–E). Normally neural crest migration is observed to start around the 4–5th last somites, however, when neural tubes were electroporated with either of the two types of Slit2-MO, neural crest cells were observed as early as in 2nd to last somites (arrows in Fig. 7B, D). Electroporation at older stage (HH16) with Slit2 morpholinos confirmed these results; we observed in sections what would be the consequence of earlier migration: more FITC-positive cells in condensing DRG (data not shown and Supplementary Fig. 2). Enhanced migration was frequently observed bilaterally because ~50% of embryos electroporated with either control or Slit2 morpholinos stained positively for MO-expression in both halves of the neural tubes. This is likely due to the net neutral charge of morpholinos.

This phenomenon of enhanced migration was observed in 71% of embryos (N=35) compared with control morpholinos where early migration was observed in only 15% of embryos (N=40). We corroborated these qualitative observations using a double-blind assessment. Furthermore, S2-MO electroporated neural tubes showed more delaminated cells compared with control, as well as many more HNK1-positive cells beginning migration along the ventro-medial pathway on both sides of the neural tube compared with control morpholinos at the same axial level in TrnSlit2-MO embryos (Supplementary Fig. 2A–F).

In order to further corroborate this Slit2 LOF effect we also performed rescue experiments electroporating simultaneously Slit2-MO and Slit2-GFP. Rescued embryos displayed migration patterns more similar to Slit2 GOF embryos (8/22) as compared to TrnSlit2-MO alone (Fig. 7F). Although neural crest cell migration was not as significantly impaired as in plain Slit GOF experiments, rescued embryos showed that TrnSlit2 morpholinos were capable of reducing the Slit2 GOF phenotype observed in Fig. 2.

Cultured neural tubes after electroporation with Slit2-MO also displayed an enhanced migratory type neural crest cell shape, opposite to that which was observed with Slit GOF cells (Supplementary Fig. 2G, H). TUNEL assays on MO-expressing embryos did not show any significant increase in cell death compared with control morpholinos or the un-electroporated side (data not shown).

Somewhat analogously, we observed an increase in the condensation of sympathetic chain when cells from chicken embryos were cultured in the presence of a soluble form of Robo receptor (RoboN) (Supplementary Fig. 3). RoboN is commonly utilized to block the effects

of Slit (Liu et al., 2004; Sabatier et al., 2004). In embryos cultured in ovo or ex ovo with RoboN, the sympathetic ganglia condensed earlier than control embryos (Supplementary Fig. 3B, N=14 embryos) and in 50% of the embryos, the migration of neural crest cells was disrupted morphologically compared to control embryos (data not shown). RoboN-treatment also facilitated neural crest cell migration at the most caudal somites (El-Ghali et al., 2009). These in vivo and ex ovo results were substantiated by culturing neural tubes in the presence or absence of RoboN-conditioned media (Supplementary Fig. 3 C–E). RoboN-exposed neural crest cells migrated farther away (50% wider halo) from the neural tube when compared to controls, demonstrating their enhanced migration capabilities (N=22 neural tubes) (Coles et al., 2007; Taneyhill et al., 2007).

Altogether the data for Slit ligands or Robo receptors confirm that Slit and Robo both play an important role in neural crest cell migration.

Slit molecules affect expression of cytoskeletal molecules

The above results suggested that Slit expression might play a role in the cellular changes accompanying the transition of neural crest cells from an epithelial to a mesenchymal cell type. If this was the case, one would expect to observe changes in the overall distribution of the cell's cytoskeleton (Gundersen et al., 1987). We discovered that expression of mSlit1 and hSlit2 altered the expression pattern of acetylated tubulin (a stable cell cytoskeletal marker) (Piperno et al., 1987) while control GFP- or MIF-expressing cells did not display such an effect (data not shown for MIF) (Fig. 8A–C). In control-GFP and mSlit1 electroporated neural tubes, the acetylated tubulin was readily observed only in neuroepithelial cells (non-motile). However, after Slit GOF migrating neural crest cells expressing mSlit1 displayed high levels of acetylated tubulin (Fig. 8C and F). Interestingly, neural tubes electroporated with Slit2-MO also displayed marked levels of acetylated tubulin (Fig. 8J).

These results suggested that cytoskeletal rearrangements occur in neural crest cells dependent on Slit expression. We looked further into this possibility by immunostaining neural tube cultures after Slit electroporation. We corroborated that Slit GOF was capable of altering cytoskeletal organization of cultured neural crest cells (Fig. 9). For example, the microtubule organizing center (MTOC) in about 50% of Slit2-electroporated cells was much less prominent than in controls (arrows in Fig. 9G, H). Similarly, the pattern of actin distribution was also altered when comparing controls to Slit2-expressing cells. In Slit GOF cells, neural crest cells exhibited fewer actin stress fiber and more membrane-associated cortical actin compared with controls (Fig. 9I–P).

To confirm these findings, we transfected Slit into a cell line very similar to neural crest cells (Buchstaller et al., 2004). We observed the same range of cytoskeletal changes as in neural crest cells after Slit GOF, including reorganization of acetylated tubulin and actin fibers and reduced levels of tyrosinated tubulin (Supplementary Fig. 4 and data not shown). These results suggest that the findings were not due to spurious effects associated with the culturing of electroporated primary neural tube cells.

Finally, we tested the effect of Slit2-MO on the distribution of acetylated tubulin and actin filaments. Acetylated tubulin fibers were widespread throughout the cell cytoplasm in control neural crest cells while neural crest cells expressing the Slit2-MO displayed very prominent fibers, with heavy concentration of acetylated tubulin into the MTOC (arrows in Fig. 10A–D). In addition, neural crest cells expressing Slit2-MO exhibited an increase in actin stress fibers compared to control cells (arrows in Fig. 10E–H). Thus, both the Slit GOF and LOF experiments suggest that Slit expression results in alterations in cytoskeletal components that may be necessary for cell migration.

DISCUSSION

Slit chemorepellant molecules were initially described by their involvement in axon and cell guidance. However, recently Slit molecules have also been implicated in trigeminal condensation and cancer metastasis (Dallol et al., 2003b; Shiau et al., 2008). The present paper examined whether or not Slit molecules play a different role in neural crest cell development, similar to its inhibition of migration in metastatic cells. Our findings demonstrate that in addition to being neural crest chemorepellants, Slit molecules are capable of impairing neural crest cell migration.

Slit molecules impair neural crest migration

The process of cell migration is extremely complex because it entails coordination of many seemingly opposing cell functions. Cells need to become polarized, make adequate plasma membrane protrusions and generate traction while simultaneously retracting the cell body. Our findings herein that Slit expression significantly impaired the movement of actively migrating neural crest cells suggests that Slit molecules not only command where neural crest cells will migrate (De Bellard et al., 2003), but also impair the process of initial migration from the neural tube that allows them to become a highly migratory cell.

Our findings highlight a critical and highly debated question regarding neural crest cell migration: how can one distinguish a simple guidance phenomenon from a migratory or motility phenomenon in a highly migratory mesenchymal cell? Neural crest cells begin to migrate rapidly and persistently along set pathways after delaminating from the neural tube, suggesting a carefully guided developmental process (Kulesa et al., 2004; Hall, 2009; Kulesa and Gammill, 2010). Our present results support a new role for Slit molecules during neural crest cell development. One, Slit molecules provide guidance by preventing neural crest cells from entering regions with high concentrations of Slit molecules (De Bellard et al., 2003). Two, Slit molecules can delay and impair the initiation of neural crest migration (see cartoon in Fig. 11). Thus, Slit molecules not only behave as guidance ligand molecules (telling cells where to go), but are also capable of affecting cell motility (how/if cells reach those targets).

Several key observations support this hypothesis. First, during Slit GOF, neural crest cells migrated less efficiently away from the Slit expressing neural tube, undermining the idea that Slit solely has a role in guidance in a gradient dependent manner. Instead during Slit GOF cells migrated very poorly along their regular ventral pathway or away from the neural tube in culture. However, not all the Slit GOF neural crest cells showed impaired migration. Some Slit-expressing cells still reached their targets in the embryo or the halo edge in culture. Second, we also observed that after Slit GOF, cells were dynamically changing their shape and rounding up, which is a less motile phenotype. Together, these observations point towards a role for Slits during the initiation of migration separate from their role in guidance. While some authors think that cells first undergo guidance then migration (Chodniewicz and Klemke, 2004), others have shown that many cells can polarize spontaneously in the absence of concentration gradients (Paliwal et al., 2004). In fact, neural crest cells will vigorously migrate in culture despite lack of guidance cues (even demonstrating spontaneous migration after neural tube removal). Thus neural crest cells are capable of migrating without guidance cues. In other words, neural crest cell migration very likely entails separable guidance and motility mechanisms.

More relevant to our present findings is that recently Slit2 has now been found to be expressed in solid tumors (Wang et al., 2003) and unmethylated-Slit2 can behave as a tumor suppressor and impair cell migration in some human cancers (Prasad et al., 2008). It looks as if Slits molecules are important in the transition towards a migratory type in some

mesenchymal cells. In other words, in the same way that Slits impair, or better, restrain cancer cell migration, they can also restrain the process of neural crest migration. Although the data presented here cannot determine if it is at the initiation of cell migration, when neuroepithelial cells change their phenotype or after this step, we showed that Slit-Robo interactions are part of this transition.

Slit molecules affect neural crest cytoskeleton

Cellular morphology and cell shape are highly dependent on cytoskeletal elements such as filamentous actin (F-actin). In vitro, epithelial neural crest cells display significant levels of F-actin fibers, with minimal cytosolic globular actin (Newgreen and Minichiello, 1995). Upon initiation of EMT, levels of F-actin decrease while cytosolic globular actin levels increase (Newgreen and Minichiello, 1995). Data presented here suggests that expression of Slit2 affects the pattern of actin distribution in neural crest cells. In highly motile neural crest cells, actin localized to areas of membrane blebs and at sites of filopodial extension, with the greatest actin staining visible when filopodial retraction occurred (Bernt et al., 2008). Here, we found that when neural crest cells expressed Slit2, fewer stress fibers were visible and in general, actin distribution did not follow the classic patterns observed in mesenchymal cells. In contrast, during Slit LOF more stress fibers were observed and cortical actin increased on cellular extensions compared with controls, reminiscent of highly motile cells (Pellegrin and Mellor, 2007). These data suggest that decreases in Slit-expression result in alterations in actin more reminiscent of a mesenchymal phenotype.

We also observed that expression of Slit could affect the distribution pattern of another important cytoskeletal protein: tubulin. The pattern of cytoplasmic distribution of post-translationally modified tubulins, acetylated tubulin (Ac-tubulin) and tyrosinated tubulin (t-tubulin) were altered upon ectopic expression of mSlit1 and hSlit2. Similar to our observations for actin, mSlit1 expression in neural crest cells resulted in condensed fibers of Ac-tubulin, as is found in less motile cells. Although the precise roles of Ac-tubulin in development have yet to be defined, the developmental regulation of post-translationally modified tubulin has been previously described (Fukushima et al., 2009). Ac-tubulin is observed in highly stable microtubules, such as those in the proximal sites of mature neurons and non-mesenchymal cells (Brown et al., 1993) as well as in non-motile types of cells (Geuens et al., 1986; Gundersen et al., 1987). One explanation for the observed changes in distribution of Ac-tubulin after Slit GOF is that Slits may promote stability of the cell cytoskeleton in the pre-migratory neural crest. Complementing these results, Slit2 LOF reduced and redistributed the total number of cytoplasmic Ac-tubulin fibers, concomitantly increasing the concentration of acetylated tubulin in the MTOC.

Probably more relevant to our findings is that recently Slit2 has been found to increase E-Cadherin and decrease beta-catenin (Tseng et al., 2010), both key components of cell structural dynamics. Both of these findings were observed in the context of cancer metastasis transitions. It is known that the EMT transformation of the neural crest is accompanied by changes in cell adhesion molecules (Nakagawa and Takeichi, 1998), which are remarkably similar to those that occur during metastasis. In addition, when Okamoto and co-workers over-expressed Slit2 in one-cell zebrafish embryos, an impairment of the convergent-extension movement of the mesoderm was observed (Yeo et al., 2001). These findings are similar to the findings we present here. Slit molecules impaired/altered the transition of neural crest cells from a non-migratory to a migratory, mesenchymal cell.

One interesting finding from Slit GOF experiments was the observation that neural crest cells showed a higher incidence of membrane blebbing. This phenomenon is believed to be actively generated by alterations in the actin cytoskeleton during neural crest delamination. More importantly, membrane blebbing protrusive activity has been shown to be concomitant

with neural crest cells EMT (Berndt et al., 2008). Our findings that Slit molecules increased cell blebbing suggest that Slit molecules may cause actin detachment from cell membrane as observed by Berndt and co-workers.

There are several findings that highlight the complexity and importance of Slit-Robo interactions. One came from screening for genes responsible for axonal regeneration. In this study, Chisholm and co-workers found that Slit-Robo interactions play a modulatory, critical step in the capability of neurons to regenerate by affecting downstream signals required for the cytoskeletal assembly during neurite outgrowth (Chen et al., 2011). Also, it is known that Slit molecules via its Robo receptor are capable of altering the expression of small GTPases like Rho, Cdc42 and Rac, which are responsible for cytoskeletal re-arrangements (Wong et al., 2001; Yiin et al., 2009; Huang et al., 2011). These molecules are known to be important not only in the cytoskeletal re-arrangements necessary during migration but, importantly during the initiation of neural crest cell migration (Wong et al., 2001; Werbowetski-Ogilvie et al., 2006; Yiin et al., 2009). This data in conjunction with the more recent description of the role that FGF and RA have on the timely delamination of neural crest brings the interesting point that the rostro-caudal complementary expression of Robo1 and Robo2 may be also play a role in the timely delamination of trunk neural crest (Martínez-Morales-2011).

There are two possible mechanisms that could explain our results. One will be the "sandwich" model proposed by Kraut and Zinn, of an anti-migratory effect of Slit-Robo signaling on sensory neurons observed in the fly embryo (Kraut and Zinn, 2004). Although the model proposed there might also apply to cells while still inside the neural tube, because it allows trans-signaling between two pre-migratory neural crest cells; with one presenting Slit to the other via binding to its Robo receptors (Fig. 11A); we think the role of Slits are more complex. One important reason is that although in that paper the Slit sandwich model is sufficient to prevent migration of sensory neurons in Drosophila, in neural crest is not sufficient. This is because we observed that neural crest cells were capable of delaminating and migrating even while constitutively expressing high levels of Slits in vivo and in vitro; albeit their motility was restrained. The other mechanism will be the axon regeneration inhibition proposed by Chisholm et al., where they proposed a cell autonomous role for Robo-Slit in inhibiting growth cone re-growth (Chen et al., 2011). We think this model explains better why neural crest expressing both Slit and Robo simultaneously, could not move as freely as control cells; and follows more our preliminary findings that Slit GOF and LOF alter neural crest EMT transition and induces cytoskeleton re-arrangements (Fig. 11C and data not shown).

The novelty of the work presented here is that it addresses an earlier aspect of neural crest cell migration, naming the time of delaminating from the neural tube and it unravels a new function for in that control for Slit/Robo system. In summary, we can propose two functions for Slit molecules during neural crest development. The first established effect of Slits is analogous to their effect on axonal pathfinding: cells avoid areas expressing Slit like the dermomyotome (Fig. 11B with 1 vs 2 paths depending on Slits) (Jia et al., 2005) and the gut (Fig. 11C) (De Bellard et al., 2003). The second effect pertains to its effect in impairing neural crest timely delamination (Fig. 11A).

EXPERIMENTAL PROCEDURES

In situ hybridization

Chicken embryos were fixed in 4% paraformaldehyde (PFA) overnight before being stored in 0.1 M Phosphate Buffered Saline (PBS). Patterns of gene expression were determined by whole-mount in situ hybridization using DIG-labeled RNA antisense probes as previously

described (Henrique et al., 1995). The cSlit1, cSlit2 and cRobo1 probes used are described in (De Bellard et al., 2003) and Sox10 in (Cheng et al., 2000).

Electroporation with Slit or Robo

A 3mg/ml solution of DNA (pMES-GFP, pMES-Slit2, pCS2-GFP, pCS2-mSlit1 or pCS2-hSlit2) was injected into the chicken embryos neural tubes using a mouth pipette and immediately electroporated with two 50 ms pulses of 25 mV each. Embryos were sealed with tape and re-incubated for 1–2, 24 or 48 hrs until fixation or neural tube culture.

A 100uM solution of morpholinos (MO) was injected into the embryo and electroporated as above. The morpholinos were prepared for translational blocking chicken Slit2 (5′ GGAGCCTCCCCCAGGCGCACATCAT 3′), standard control scrambled (5′ CCTCTTACCTCAGTTACAATTTATA 3′), splice blocking chicken Slit2 (5′ GGGACACAAATGTGACTCACAATGT 3′), and splice scramble control chicken Slit2 (5′ GG**C**ACA**G**AAAT**C**TGACTCA**G**AAT**C**T 3′) by GeneTools, LLC. (Oregon, USA). All morpholinos were tagged with Fluorescein at the 3′ end of the oligo. A specific splice scramble control chicken Slit2 was created by using the splice blocking chicken Slit2 sequence but included 5 base pair mismatches (Bold nucleotides). Slit2-MO specificity was determined after transfecting cSlit2-MO on a hSlit2 permanent cell line. Western blot analyses revealed a ~50% reduction of Slit2 in these Slit2-expressing cells. A hSlit2-GOF experiment demonstrated a ~50% increase in the amount of Slit2 observed.

In vitro neural crest culture

Chicken neural tubes were isolated by incubating trunks in 1.5mg/ml of Dispase for 30–60 min, followed by dissecting neural tubes into small pieces and culturing on Fibronectin coated Nunc-glass chamber slides for 18 hrs in Dulbecco's Modified Eagle Medium (DMEM), 10% fetal bovine serum (FBS) and 100mg/ml and 100U of penicillin and streptomycin respectively. Samples were then fixed in 4% PFA. For immunostaining, cultures were blocked for 30min with PBS, 1% Triton-X100, 10% serum. Primary antibodies were directed against HNK1 or GFP (Invitrogen) for visualizing neural crest cells. Acetylated Tubulin and Actin antibodies were from purchased from Sigma; NCad and Cad6b from DSHB, Tubulin antibodies were from Chemicon. Secondary antibodies were anti-mouse or anti-rabbit-Alexa 488/594 (Molecular Probes). DAPI was used to visualize cell nuclei.

Whole mount immunofluorescence

After overnight incubation in blocking buffer PBS with 1% Triton-X100, 10% serum, electroporated embryos were incubated with 1:100 HNK1 supernatant in PBS overnight at 4°C, then were extensively washed with PBS and incubated with an anti-mouse IgM- Alexa 488/594. Embryos were washed extensively in PBS and photographed using Zeiss A-1 AxioImager.

Time lapse video microscopy

The neural tubes of chicken embryos were electroporated with pMES-GFP or pMES-Slit2. After 1–2hrs at 38°C, neural tubes were isolated and cultured as described previously. The next day, cells were imaged using a Zeiss 410 LSM every 90 seconds for approximately 3 hours. The captured images were converted into a QuickTime movie with NIH ImageJ and analyzed with GoFigure (https://wiki.med.harvard.edu/SysBio/Megason/GoFigure).

Ex Ovo embryo culture

Chicken embryos were cultured as described previously (El-Ghali et al., 2009). Briefly, embryos are cultured outside of the embryo on a filter ring containing approximately 3ml conditioned culture media (specifically, from 293HEK cells expressing Slit2 or controls) at 37°C in a CO_2 incubator (5%) for 24 hrs until fixation and wholemount staining.

Cell and neural tube transfection

Cell cultures of SpL201 (Lobsiger et al., 2001) or dissected neural tubes were transfected with Lipofectamine 2000 (Gibco) following manufacturer's instructions. In the case of neural tubes, cells were cultured for 3hrs to allow proper attachment of dissected neural tubes. Cells were then treated with lipofectamine mixtures containing plasmids (pMES-Slit2, pMES-GFP or pCIG-MIF) and incubated until the next day when cells were fixed and blocked. After antibody staining with anti-GFP and/or HNK1, cells were traced using the "area measurement" tool from Zeiss LE AxioVision Rel 4.8 program and cell areas were recorded. Primary antibodies were directed against HNK1 or GFP (Invitrogen) for visualizing neural crest cells. Acetylated Tubulin and Actin antibodies were from purchased from Sigma; Secondary antibodies were anti-mouse or anti-rabbit-Alexa 488/594 (Molecular Probes). DAPI was used to visualize cell nuclei.

RT-PCR analysis of Splice blocking morpholinos

Chicken embryos at St. HH13-14 were electroporated on both sides of the neural tube with injected Splice mismatch control morpholino and Splice blocking Slit2 morpholino with electrodes on either side of the neural tube 5mm apart. 5 pulses at 18.0V 100ms on 50ms off. Embryos were incubated at 37C for 24hpe. Embryos were removed and rinsed in ice cold ringers before placed in ice cold L15 media for dissection of neural tubes. Neural tubes were placed into RNAlater (Ambion) and stored at −20C. RNA was isolated from neural tubes using the GeneJet RNA purification kit (Fermentas) and recommended protocol. Subsequently we perform RT-PCR using the Superscript III one step RT-PCR system with platinum TAQ DNA polymerase (Invitrogen). SuperScript Vilo cDNA synthesis kit (Invitrogen) is used to amplify cDNA products. Apex Taq DNA polymerase Master mix (Genesee Scientific) is used to amplify cDNA products. Samples are run on a 2% agarose gel (length 7cm) at 35V for 3hrs with Nanodrop DNA concentrations at ~2ug/ul.

Supplementary Material

Refer to Web version on PubMed Central for supplementary material.

Acknowledgments

References

Berndt JD, Clay MR, Langenberg T, Halloran MC. Rho-kinase and myosin II affect dynamic neural crest cell behaviors during epithelial to mesenchymal transition in vivo. Dev Biol. 2008

Brose K, Bland KS, Wang KH, Arnott D, Henzel W, Goodman CS, Tessier-Lavigne M, Kidd T. Slit proteins bind Robo receptors and have an evolutionarily conserved role in repulsive axon guidance. Cell. 1999; 96:795–806. [PubMed: 10102268]

Brown A, Li Y, Slaughter T, Black MM. Composite microtubules of the axon - Quantitative-analysis of tyrosinated and acetylated tubuling along individual axonal microtubules. Journal of Cell Science. 1993; 104:339–352. [PubMed: 8505364]

Buchstaller J, Sommer L, Bodmer M, Hoffmann R, Suter U, Mantei N. Efficient isolation and gene expression profiling of small numbers of neural crest stem cells and developing Schwann cells. J Neurosci. 2004; 24:2357–2365. [PubMed: 15014110]

Chen L, Wang Z, Ghosh-Roy A, Hubert T, Yan D, O'Rourke S, Bowerman B, Wu Z, Jin Y, Chisholm AD. Axon regeneration pathways identified by systematic genetic screening in C. elegans. Neuron. 2011; 71:1043–1057. [PubMed: 21943602]

Cheng Y, Cheung M, Abu-Elmagd MM, Orme A, Scotting PJ. Chick sox10, a transcription factor expressed in both early neural crest cells and central nervous system. Brain Res Dev Brain Res. 2000; 121:233–241.

Chodniewicz D, Klemke RL. Guiding cell migration through directed extension and stabilization of pseudopodia. Exp Cell Res. 2004; 301:31–37. [PubMed: 15501442]

Coles EG, Taneyhill LA, Bronner-Fraser M. A critical role for Cadherin6B in regulating avian neural crest emigration. Dev Biol. 2007; 312:533–544. [PubMed: 17991460]

Dallol A, Da Silva NF, Viacava P, Minna JD, Bieche I, Maher ER, Latif F. SLIT2, a human homologue of the Drosophila Slit2 gene, has tumor suppressor activity and is frequently inactivated in lung and breast cancers. Cancer Res. 2002; 62:5874–5880. [PubMed: 12384551]

Dallol A, Krex D, Hesson L, Eng C, Maher ER, Latif F. Frequent epigenetic inactivation of the SLIT2 gene in gliomas. Oncogene. 2003a; 22:4611–4616. [PubMed: 12881718]

Dallol A, Morton D, Maher ER, Latif F. SLIT2 axon guidance molecule is frequently inactivated in colorectal cancer and suppresses growth of colorectal carcinoma cells. Cancer Res. 2003b; 63:1054–1058. [PubMed: 12615722]

De Bellard ME, Rao Y, Bronner-Fraser M. Dual function of Slit2 in repulsion and enhanced migration of trunk, but not vagal, neural crest cells. J Cell Biol. 2003; 162:269–279. [PubMed: 12876276]

Dickinson RE, Dallol A, Bieche I, Krex D, Morton D, Maher ER, Latif F. Epigenetic inactivation of SLIT3 and SLIT1 genes in human cancers. Br J Cancer. 2004; 91:2071–2078. [PubMed: 15534609]

El-Ghali N, Rabadi M, Ezin AM, De Bellard ME. New methods for chicken embryo manipulations. Microsc Res Tech. 2009

Fukushima N, Furuta D, Hidaka Y, Moriyama R, Tsujiuchi T. Post-translational modifications of tubulin in the nervous system. Journal of Neurochemistry. 2009; 109:683–693. [PubMed: 19250341]

Gammill LS, Bronner-Fraser M. Neural crest specification: migrating into genomics. Nat Rev Neurosci. 2003; 4:795–805. [PubMed: 14523379]

Geuens G, Gundersen GG, Nuydens R, Cornelissen F, Bulinski JC, Debrabander M. Ultrastructural colocalization of tyrosinated and detyrosinated alpha-tubulin in interphase and mitotic cells. Journal of Cell Biology. 1986; 103:1883–1893. [PubMed: 3782287]

Gregory JL, Morand EF, McKeown SJ, Ralph JA, Hall P, Yang YH, McColl SR, Hickey MJ. Macrophage migration inhibitory factor induces macrophage recruitment via CC chemokine ligand 2. J Immunol. 2006; 177:8072–8079. [PubMed: 17114481]

Gundersen GG, Khawaja S, Bulinski JC. Postpolymerization detyrosination of alpha-tubulin -A mechanisms for subcellular differentiation of microtubules. Journal of Cell Biology. 1987; 105:251–264. [PubMed: 2886509]

Hall, BK. The Neural Crest and Neural Crest Cells in Vertebrate Development and Evolution. New York: Springer-Verlag; 2009.

Henrique D, Adam J, Myat A, Chitnis A, Lewis J, Ish-Horowicz D. Expression of a Delta homologue in prospective neurons in the chick. Nature. 1995; 375:787–790. [PubMed: 7596411]

Holmes G, Niswander L. Expression of slit-2 and slit-3 during chick development. Dev Dyn. 2001; 222:301–307. [PubMed: 11668607]

Hu H. Chemorepulsion of neuronal migration by Slit2 in the developing mammalian forebrain. Neuron. 1999; 23:703–711. [PubMed: 10482237]

Huang ZH, Wang Y, Su ZD, Geng JG, Chen YZ, Yuan XB, He C. Slit-2 repels the migration of olfactory ensheathing cells by triggering Ca2+-dependent cofilin activation and RhoA inhibition. J Cell Sci. 2011; 124:186–197. [PubMed: 21187345]

Jia L, Cheng L, Raper J. Slit/Robo signaling is necessary to confine early neural crest cells to the ventral migratory pathway in the trunk. Dev Biol. 2005; 282:411–421. [PubMed: 15950606]

Kidd T, Bland KS, Goodman CS. Slit is the midline repellent for the robo receptor in Drosophila. Cell. 1999; 96:785–794. [PubMed: 10102267]

Kim HK, Zhang H, Li H, Wu TT, Swisher S, He D, Wu L, Xu J, Elmets CA, Athar M, Xu XC, Xu H. Slit2 inhibits growth and metastasis of fibrosarcoma and squamous cell carcinoma. Neoplasia. 2008; 10:1411–1420. [PubMed: 19048120]

Kinrade EF, Brates T, Tear G, Hidalgo A. Roundabout signalling, cell contact and trophic support confine longitudinal glia and axons in the Drosophila CNS. Development. 2001; 128:207–216. [PubMed: 11124116]

Kraut R, Zinn K. Roundabout 2 regulates migration of sensory neurons by signaling in trans. Curr Biol. 2004; 14:1319–1329. [PubMed: 15296748]

Kulesa P, Ellies DL, Trainor PA. Comparative analysis of neural crest cell death, migration, and function during vertebrate embryogenesis. Dev Dyn. 2004; 229:14–29. [PubMed: 14699574]

Kulesa PM, Gammill LS. Neural crest migration: patterns, phases and signals. Dev Biol. 2010; 344:566–568. [PubMed: 20478296]

Li HS, Chen JH, Wu W, Fagaly T, Zhou L, Yuan W, Dupuis S, Jiang ZH, Nash W, Gick C, Ornitz DM, Wu JY, Rao Y. Vertebrate slit, a secreted ligand for the transmembrane protein roundabout, is a repellent for olfactory bulb axons. Cell. 1999; 96:807–818. [PubMed: 10102269]

Liu Z, Patel K, Schmidt H, Andrews W, Pini A, Sundaresan V. Extracellular Ig domains 1 and 2 of Robo are important for ligand (Slit) binding. Mol Cell Neurosci. 2004; 26:232–240. [PubMed: 15207848]

Lobsiger CS, Smith PM, Buchstaller J, Schweitzer B, Franklin RJ, Suter U, Taylor V. SpL201: a conditionally immortalized Schwann cell precursor line that generates myelin. Glia. 2001; 36:31–47. [PubMed: 11571782]

Nakagawa S, Takeichi M. Neural crest emigration from the neural tube depends on regulated cadherin expression. Development. 1998; 125:2963–2971. [PubMed: 9655818]

Newgreen DF, Minichiello J. Control of epitheliomesenchymal transformation. I. Events in the onset of neural crest cell migration are separable and inducible by protein kinase inhibitors. Dev Biol. 1995; 170:91–101. [PubMed: 7541378]

Paliwal S, Lan M, Krishnan J, Levchenko A, Iglesias PA. Responding to directional cues: a tale of two cells [biochemical signaling pathways]. Control Systems Magazine, IEEE. 2004; 24:77–90.

Pellegrin S, Mellor H. Actin stress fibres. J Cell Sci. 2007; 120:3491–3499. [PubMed: 17928305]

Piperno G, LeDizet M, Chang XJ. Microtubules containing acetylated alpha-tubulin in mammalian cells in culture. J Cell Biol. 1987; 104:289–302. [PubMed: 2879846]

Prasad A, Paruchuri V, Preet A, Latif F, Ganju RK. Slit-2 induces a tumor-suppressive effect by regulating beta-catenin in breast cancer cells. J Biol Chem. 2008; 283:26624–26633. [PubMed: 18611862]

Sabatier C, Plump AS, Le M, Brose K, Tamada A, Murakami F, Lee EY, Tessier-Lavigne M. The divergent Robo family protein rig-1/Robo3 is a negative regulator of slit responsiveness required for midline crossing by commissural axons. Cell. 2004; 117:157–169. [PubMed: 15084255]

Salvador SM, Vernon A, LaBonne C. The role of snail family transcription factors in neural crest development and tumor progression. Developmental Biology. 2009:331.10.1016/j.ydbio. 2009.1005.1189|1167

Schmid BC, Rezniczek GA, Fabjani G, Yoneda T, Leodolter S, Zeillinger R. The neuronal guidance cue Slit2 induces targeted migration and may play a role in brain metastasis of breast cancer cells. Breast Cancer Res Treat. 2007; 106:333–342. [PubMed: 17268810]

Serbedzija GN, Bronner-Fraser M, Fraser SE. A vital dye analysis of the timing and pathways of avian trunk neural crest cell migration. Development. 1989; 106:809–816. [PubMed: 2562671]

Sharma G, Mirza S, Prasad CP, Srivastava A, Gupta SD, Ralhan R. Promoter hypermethylation of p16INK4A, p14ARF, CyclinD2 and Slit2 in serum and tumor DNA from breast cancer patients. Life Sci. 2007; 80:1873–1881. [PubMed: 17383681]

Shiau CE, Bronner-Fraser M. N-cadherin acts in concert with Slit1-Robo2 signaling in regulating aggregation of placode-derived cranial sensory neurons. Development. 2009; 136:4155–4164. [PubMed: 19934013]

Shiau CE, Lwigale PY, Das RM, Wilson SA, Bronner-Fraser M. Robo2-Slit1 dependent cell-cell interactions mediate assembly of the trigeminal ganglion. Nat Neurosci. 2008; 11:269–276. [PubMed: 18278043]

Singh RK, Indra D, Mitra S, Mondal RK, Basu PS, Roy A, Roychowdhury S, Panda CK. Deletions in chromosome 4 differentially associated with the development of cervical cancer: evidence of slit2 as a candidate tumor suppressor gene. Hum Genet. 2007; 122:71–81. [PubMed: 17609981]

Strachan LR, Condic ML. Neural crest motility and integrin regulation are distinct in cranial and trunk populations. Dev Biol. 2003; 259:288–302. [PubMed: 12871702]

Taneyhill LA, Coles EG, Bronner-Fraser M. Snail2 directly represses cadherin6B during epithelial-to-mesenchymal transitions of the neural crest. Development. 2007; 134:1481–1490. [PubMed: 17344227]

Thiery JP, Acloque H, Huang RYJ, Nieto MA. Epithelial-Mesenchymal Transitions in Development and Disease. Cell. 2009; 139:871–890. [PubMed: 19945376]

Thiery JP, Duband JL, Delouvee A. Pathways and mechanisms of avian trunk neural crest cell migration and localization. Dev Biol. 1982; 93:324–343. [PubMed: 7141101]

Tseng RC, Lee SH, Hsu HS, Chen BH, Tsai WC, Tzao C, Wang YC. SLIT2 attenuation during lung cancer progression deregulates beta-catenin and E-cadherin and associates with poor prognosis. Cancer Res. 2010; 70:543–551. [PubMed: 20068157]

Vernon AE, LaBonne C. Tumor metastasis: A new twist on epithelial-mesenchymal transitions. Current Biology. 2004; 14:R719–R721. [PubMed: 15341765]

Wang B, Xiao Y, Ding BB, Zhang N, Yuan X, Gui L, Qian KX, Duan S, Chen Z, Rao Y, Geng JG. Induction of tumor angiogenesis by Slit-Robo signaling and inhibition of cancer growth by blocking Robo activity. Cancer Cell. 2003; 4:19–29. [PubMed: 12892710]

Wang KH, Brose K, Arnott D, Kidd T, Goodman CS, Henzel W, Tessier-Lavigne M. Biochemical purification of a mammalian slit protein as a positive regulator of sensory axon elongation and branching. Cell. 1999; 96:771–784. [PubMed: 10102266]

Werbowetski-Ogilvie TE, Seyed Sadr M, Jabado N, Angers-Loustau A, Agar NY, Wu J, Bjerkvig R, Antel JP, Faury D, Rao Y, Del Maestro RF. Inhibition of medulloblastoma cell invasion by Slit. Oncogene. 2006; 25:5103–5112. [PubMed: 16636676]

Wong K, Ren XR, Huang YZ, Xie Y, Liu G, Saito H, Tang H, Wen L, Brady-Kalnay SM, Mei L, Wu JY, Xiong WC, Rao Y. Signal transduction in neuronal migration: roles of GTPase activating proteins and the small GTPase Cdc42 in the Slit-Robo pathway. Cell. 2001; 107:209–221. [PubMed: 11672528]

Wu W, Wong K, Chen J-H, Jiang Z-H, Dupuis S, Wu Ja, Rao Y. Directional guidance of neuronal migration in the olfactory system by the protein Slit. Nature. 1999; 400:331–336. [PubMed: 10432110]

Yeo SY, Little MH, Yamada T, Miyashita T, Halloran MC, Kuwada JY, Huh TL, Okamoto H. Overexpression of a Slit homologue impairs convergent extension of the mesoderm and causes cyclopia in embryonic zebrafish. Developmental Biology. 2001; 230:1–17. [PubMed: 11161558]

Yiin JJ, Hu B, Jarzynka MJ, Feng H, Liu KW, Wu JY, Ma HI, Cheng SY. Slit2 inhibits glioma cell invasion in the brain by suppression of Cdc42 activity. Neuro Oncol. 2009

Yu J, Cao Q, Wu L, Dallol A, Li J, Chen G, Grasso C, Cao X, Lonigro RJ, Varambally S, Mehra R, Palanisamy N, Wu JY, Latif F, Chinnaiyan AM. The neuronal repellent SLIT2 is a target for repression by EZH2 in prostate cancer. Oncogene. 2010

Bullet points

- Pre-migratory neural crest expresses Slit molecules

- Slit molecules affect cell cytoskeleton via Robo receptor.

- Neural crest cells cytoskeleton is re-arranged, cells become less migratory.

- Neural crest cells will not delaminate.
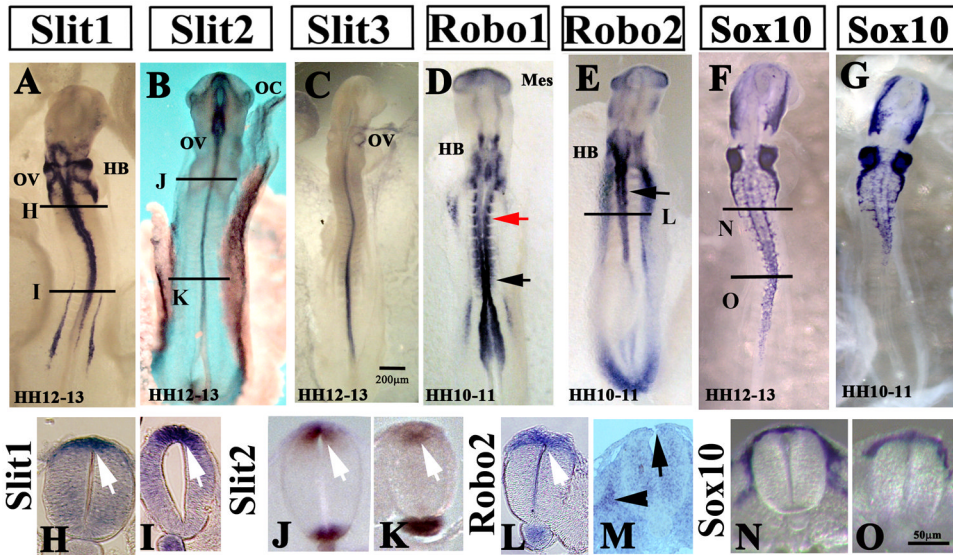
Figure 1. Slit molecules are expressed by pre-migratory neural crest cells

(**A–E**) Wholemount in situ hybridization images of chicken embryos with Slit1 (**A**), Slit2 (**B**), Slit3 (**C**), Robo1 (**D**) and Robo2 (**E**) anti-sense probes. HH12-13 chicken embryos showed expression of Slit ligands in dorsal neural tube (arrows in **H–K** sections for Slit1 and Slit2). Robo1 receptor is expressed in the medial somites (red arrow in **D**) but also in the neural tube at the most caudal portions (black arrowhead in **D**). While Robo2 receptor is expressed in the dorsal neural tube at the most rostral portion hindbrain and somites 1–10 (arrow in **E,** section in **L** of HH10-11). **M** shows Robo2 in situ section through the trunk of a HH16 embryo, highlighting that migrating trunk express Robo2 (arrowhead) while pre-migratory neural crest expresses practically no Robo2 (arrow). Sox10 in situ (**F** HH12-13, **G** HH10-11) highlight that at these stages only vagal neural crest has delaminated (**N** sections at vagal and **O** at trunk level). Bars indicate 50 or 200mm size.
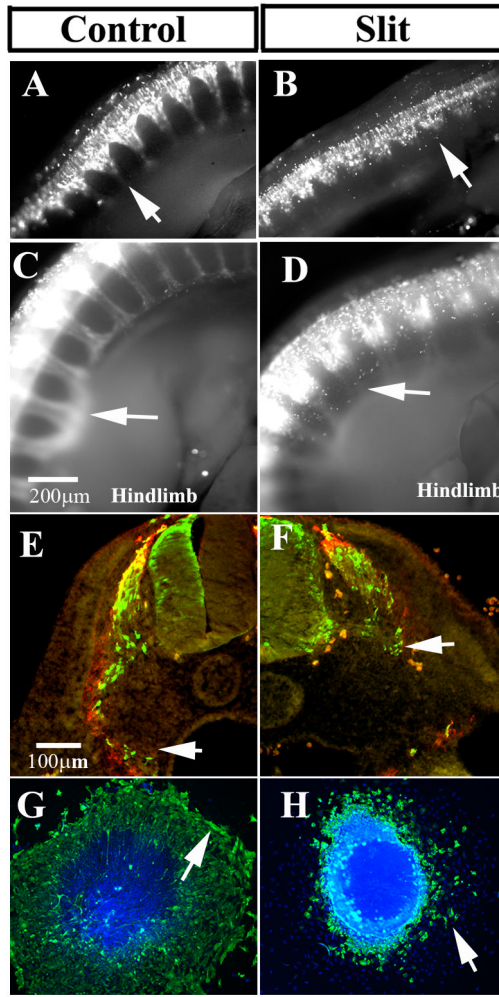
Figure 2. Slit molecules over-expression impairs neural crest cell migration
Chicken embryos HH14-15 were electroporated with control GFP (**A, C, E**) or mSlit1 (**B, F**), hSlit2 (**D**) plasmids and incubated for 24 (**A, B** arrows point to forelimb area) or 48 (**C–F** arrows point to hindlimb area) hpe. Cells were visualized with anti-GFP or anti-myc for Slit1. Neural crest cells expressing Slit1 or Slit2 did not migrate as far as in control embryos (arrows in **A–H**), and Slit electroporated cells looked rounder and less dispersed than control GFP. Sections through a 48 hpe embryo at hindlimb level showed that a larger number of control electroporated cells reached the dorsal aorta (arrow in **E**) compared with mSlit1 expressing cells (arrow in **F**). Cultures of electroporated neural tubes (bright with DAPI) showed that mSlit1-expressing cells did not migrate as far as control GFP cells (arrows in **G, H**). Cross sections were counter-stained with HNK1 (red in **E–F**).

A
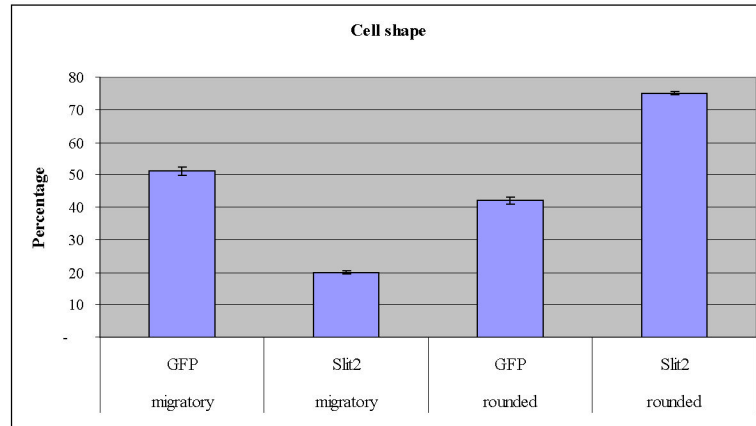
B
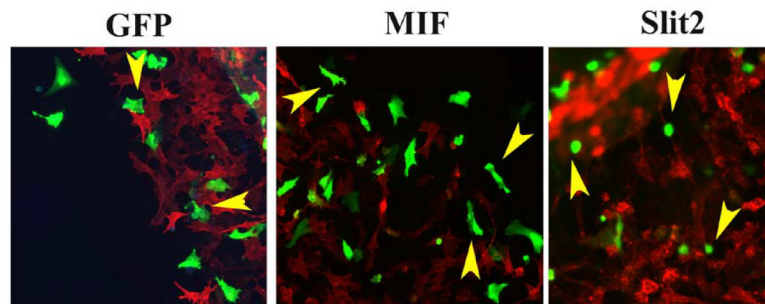
C Cell size
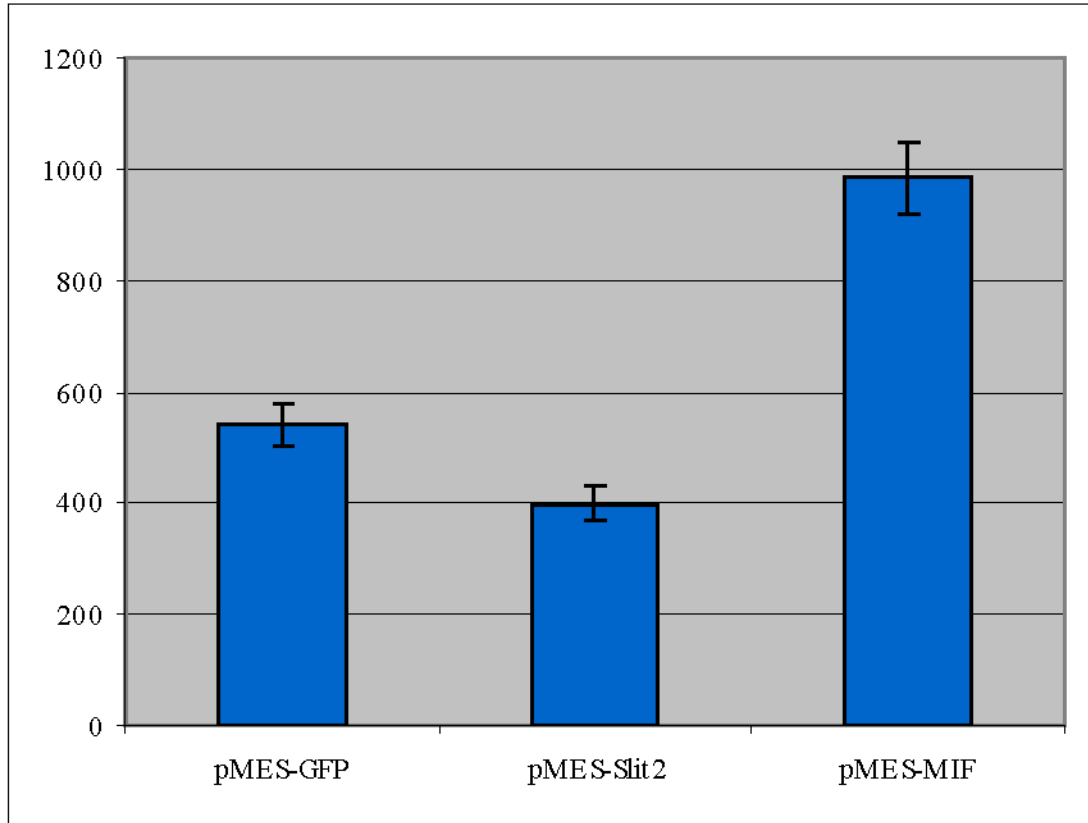
Figure 3. In vitro expression of Slit molecules impairs neural crest cell migration
Neural crest cells were cultured in vitro and chemically transfected with GFP. **A** Bar graph
scoring cell shape of neural crest cells after electroporation (T-test: p<0.005, N=680 per
each treatment). There were far fewer neural crest cells showing a migratory/mesenchymal
morphology compared with GFP cells. **B** Morphology of neural crest cells chemically
transfected with GFP, Slit2-GFP or MIF-GFP. **C** Graph showing individual cell area (y axis
corresponds to μm^2 of cell surface) for neural crest cells after transfection. Cells expressing
Slit2-GFP were significantly smaller than control-GFP or MIF-GFP expressing cells (T-test:
p<0.0004 T-test, N=60 cells per each treatment).
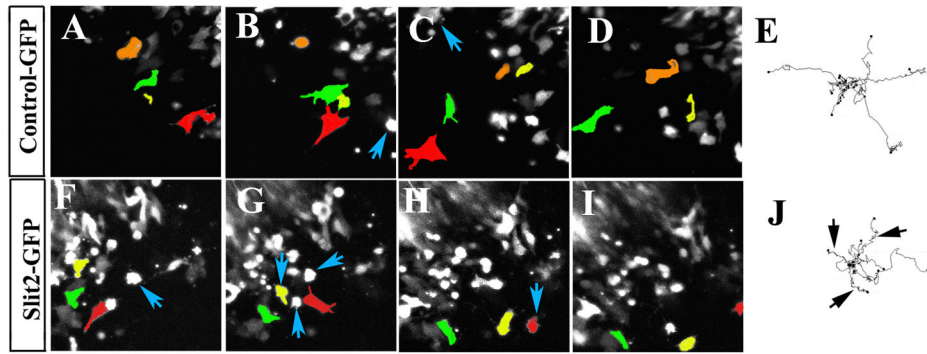
Figure 4. Aberrant migratory paths of neural crest cells shown by live imaging after Slit2 GOF
Sequential still images of movies were taken from Supplementary Movie 1 and 2. Three cells were pseudo-colored to highlight their path during the movie. Notice how the red-labeled cell in control movie moved across the field (**A–C**) and then disappeared (**D**). Neural crest cells expressing Slit stopped more frequently to round up than control cells (blue arrows **B–C** and **F–H**). Cell trackings from several movies were overlapped to characterize migratory behavior (**E** and **J**). While control electroporated cells moved farther away, Slit2 cells showed shorter and more tortuous paths (black arrows **J**) than control cells. Interestingly, while Slits cells showed impaired migration. Slit2: 53±63 um/hr (N=14) and GFP controls: 39±52.39 um/hr (N=16), p<0.45 unequal variance T-test.
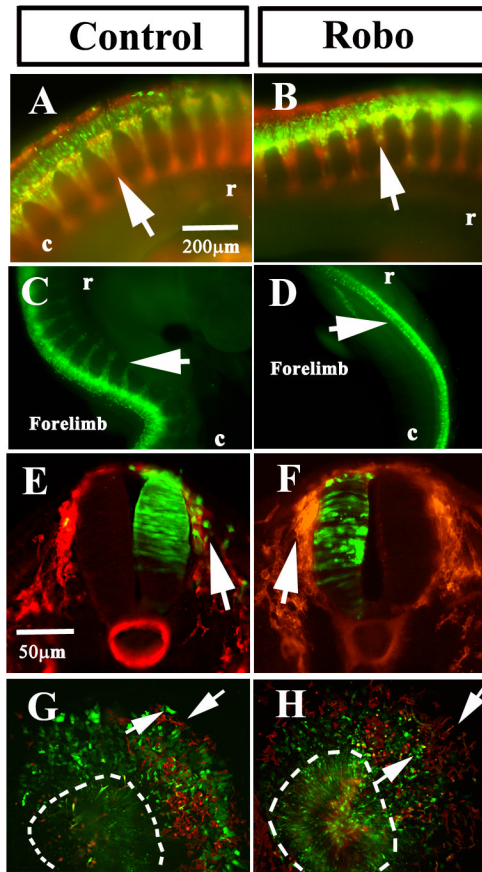
Figure 5. Robo receptor over-expression impairs neural crest cell migration
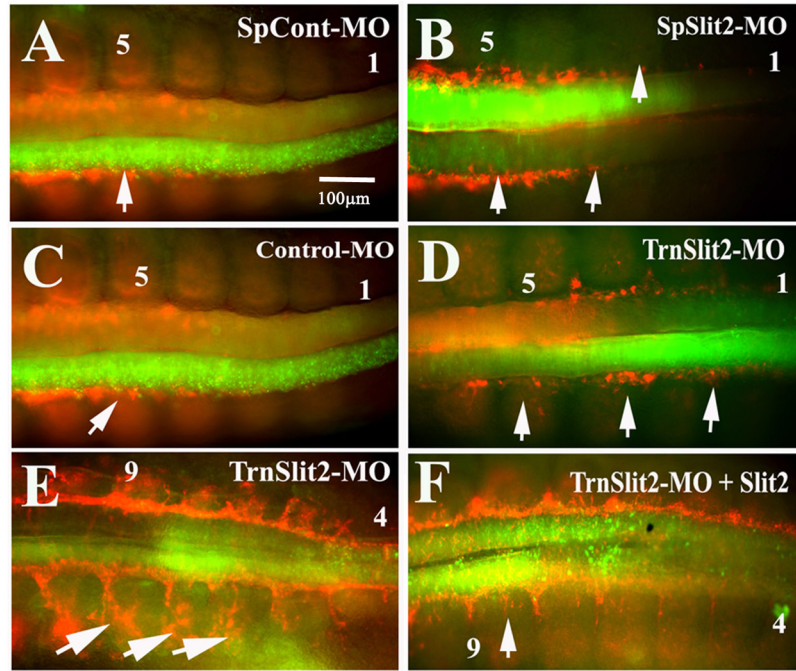Chicken embryos HH14-15 were electroporated with control-GFP or Robo1-GFP plasmids
and incubated for 24 (**A, B**) or 48 (**C–D**) hpe. Neural crest cells expressing Robo1 did not
migrate as far as in control embryos (arrows in **A–H**). Sections through a 24 hpe embryo at
midtrunk level showed a larger number of control electroporated cells in the dorsal root
ganglion area (arrow in **E**) compared with none in Robo1 section (arrow in **F**). Cultures of
electroporated neural tubes showed that Robo1 cells could not migrate as far as control GFP
cells (arrows in **G, H**). Embryos, cultures in **A–B**, **E–H** were counter-stained with HNK1
(red).



A
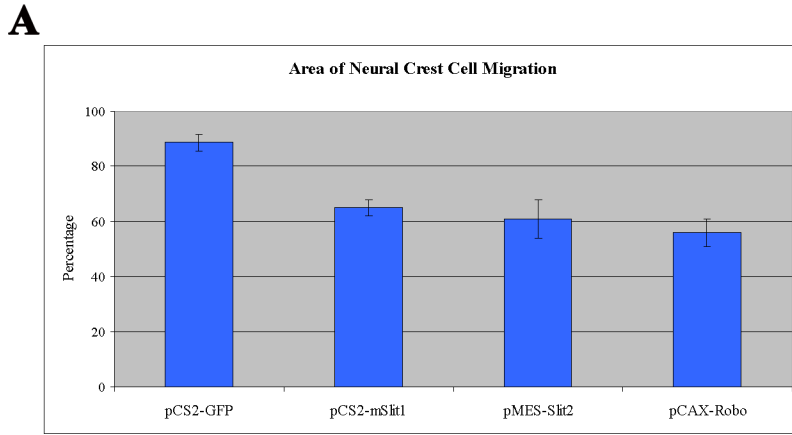
B
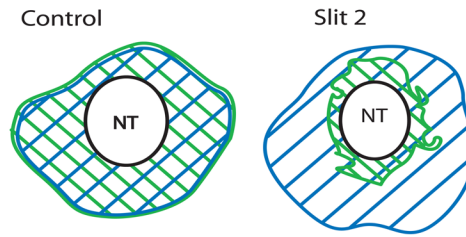
Figure 6. Quantification of in vitro Slit2 and Robo GOF effects on neural crest cell migration
A Neural tubes of chicken embryos HH14-15 were electroporated with control GFP, mSlit1 or hSlit2, or Robo1 plasmids, isolated and cultured overnight before fixing and measuring the total area covered by transfected cells normalized with total area covered by all cells as assessed by DAPI (**B**). Bar graph shows that neural tubes electroporated with mSlit1, hSlit2 and Robo1 had a ~30% reduction in total migration area compared with control GFP. N=20 neural tubes per treatment. Robo1 (56%), mSlit1 (65%) or hSlit2 (61%) control GFP-expressing (88%), T-test: p<0.005. Cartoon in **B** illustrates how we measured the total area (blue striped area) and transfected cells (green stripes) and how it looked for control GFP or Slit2 GOF experiments.

Figure 7. Slit2 loss of function enhances neural crest cell migration

Tail end of chicken embryos HH16 that were electroporated with splice Slit2 control (SpCont-MO) FITC, splice Slit2 (SpSlit2-MO), translational Slit2 (TrnSlit2-MO) or standard control morpholinos and incubated for 24 hpe (**A–F**). Neural crest cell migration in Slit2 morpholinos was present even in somite No.2 (see arrows pointing to earlier migration of HNK1 stained neural crest cells in **B** and **D**), way in advance compared with both types of control morpholinos (arrows pointing to normal migration in **A** and **C**). Rescue experiments by doing double electroporation of TrnSlit2-MO and Slit2 plasmid (**F**) showed that neural crest migration was now more similar to control levels compared with a TrnSlit2-MO alone (**E** that showed many migrating crest in somite 4). This behavior was more prominent when looking at migrating neural crest cells in the 9th somite (arrows).
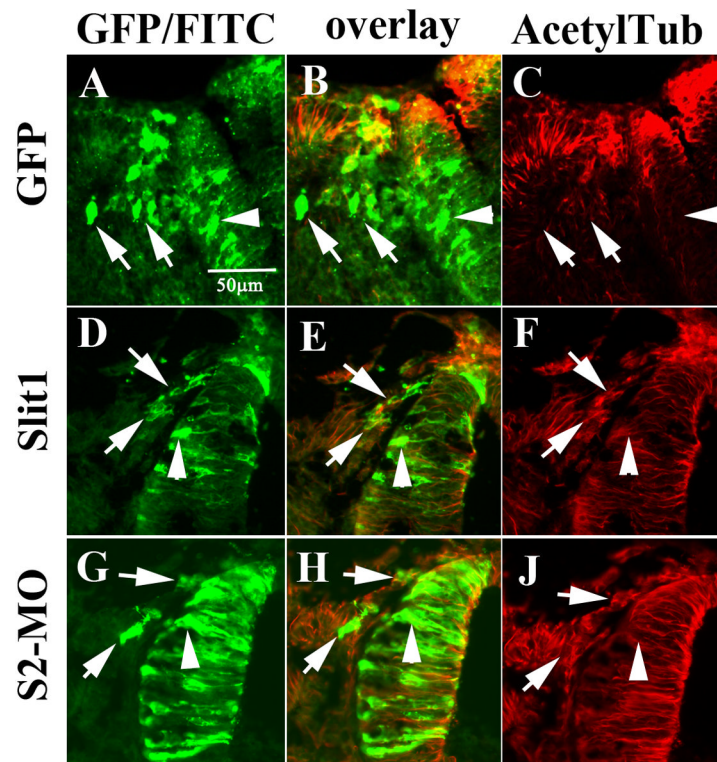
**Figure 8. Slit molecules affect the cytoskeleton in the neural crest**
Sections through midtrunk region of chicken embryos HH13-15 electroporated with control-
GFP (**A–C**), mSlit1-myc (**D–F**), or Slit2-MO (**G–J,** TrnS2-MO) were stained with anti-
acetylated tubulin. Control GFP migrating neural crest cells did not express acetylated
tubulin (**B**), while Slit1 did (**E**). Migrating S2-MO neural crest cells had lower staining of
acetylated tubulin (**H**). interestingly, S2-MO neural tube cells also showed reduced level of
acetylated tubulin (arrowhead in **G–H**) compared with Slit1 neural tube cells (arrowhead in
D–F).
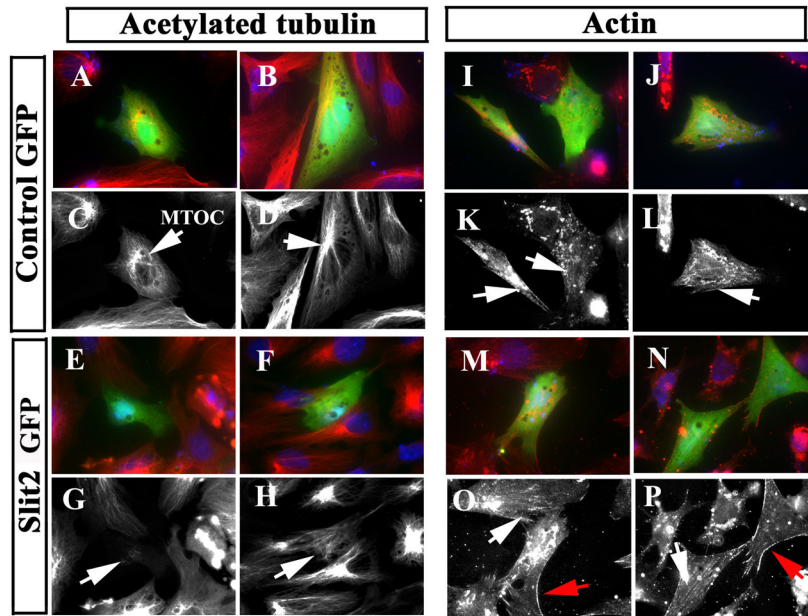
Figure 9. Slit molecules affect expression of cytoskeletal markers in the neural crest
Neural tubes were cultured and simultaneously transfected with Control or Slit2-GFP plasmids and stained for acetylated tubulin (**A–H**) and actin (**I–P**) shown in red channel or grayscale. Slit2 induced cytoskeletal re-arrangements in neural crest cells (**E–H, M–P**). While control-GFP showed normal microtubule organizing centers close to the nucleus (MTOC arrows in **C, D**), Slit2-expressing cells did not have such arrangement (arrows in **G, H**). Actin cytoskeleton in control-GFP cells showed stress fibers of migratory cells (arrows in **K,** L and **O**), while Slit2-expressing cells showed fewer stress fibers or none at all (arrows in **O, P**), in addition, they have more cortical actin than control cells (red arrows in **O, P**).
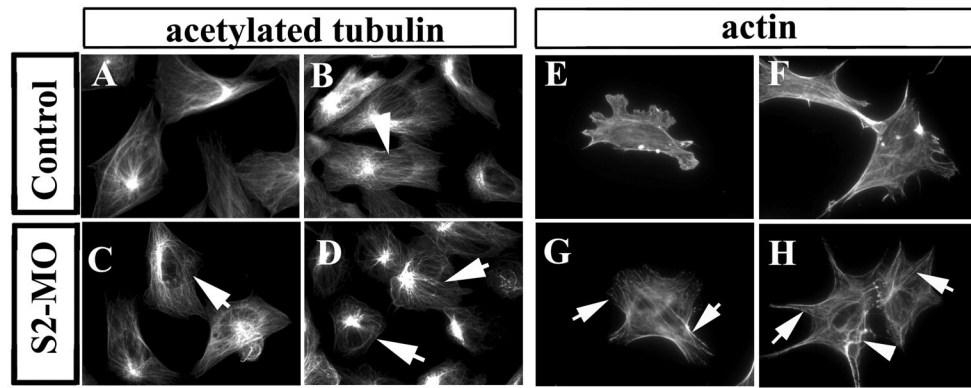
Figure 10. Slit2 morpholinos affect expression of cytoskeletal markers in the neural crest
Neural tubes were cultured after electroporation and stained with acetylated tubulin (**A–D**) or actin (**E–H**). Although most Slit2-MO neural crest cells have normal cytoplasmic distribution of microtubules and of their MTOC, the tubulin fibers were less diffuse (arrows in **C, D**) than in control cells (arrowhead in **B**). Actin cytoskeleton in S2-MO expressing cells showed more stress fiber (arrows in **G, H**) compared with controls. Less frequently we found abnormal actin fiber organization (arrowhead in **H**).
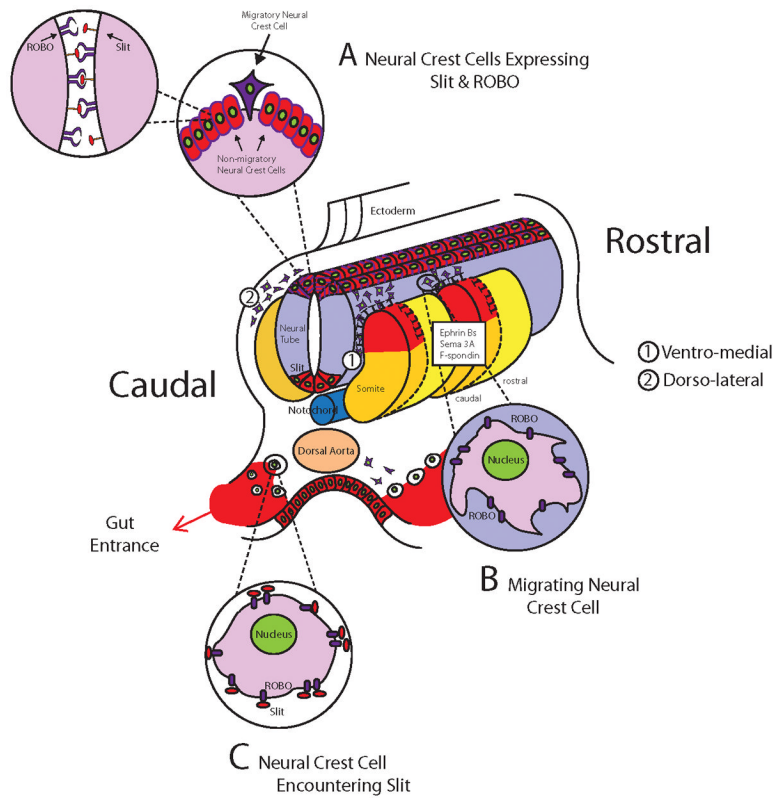
Figure 11. Graphical Abstract of Slit function during trunk neural crest migration
Cartoon showing the expression of Slits (red) and Robo receptors (blue) during trunk neural crest development. **A** Represents a pre-migratory neural crest cells that simultaneously expresses Slit and its Robo receptors, these cells are not motile. **B** Represents a migrating neural crest cells that expresses Robo receptors but no Slit, these are highly motile cells avoiding dermomyotome (Jia et al., 2005). **C** Represents neural crest cells expressing Robo receptors stopping by the dorsal aorta after encountering Slit molecules expressed at the entrance of the developing gut, these cells are non-motile, non-epithelial (De Bellard et al., 2003).

Table I

Percentage of GFP cells in ganglia

Percentage of GFP-positive cells per DRG			
	Control	**Slit1**	**Robo**
Average	100.00	51.08 **	23.95 **
SEM	14.58	9.15	4.42
N	21	15	9

Percentage of GFP-positive cells in SG		
	Control	**Slit1**
Average	100.00	36.59 *
SEM	10.96	15.07
N	17	13

The total number of GFP cells present in either DRG or sympathetic ganglia (SG) were counted in consecutive serial sections so make sure we were counting one DRG or SG. The numbers were normalized to control average levels.

*
p<0.003

**
p<0.0005